doi:10.1246/cl.2012.444
Published on the web April 4, 2012

Electrochemical Impedance Analysis on Degradation of Commercially Available Lithium Ion Battery during Charge–Discharge Cycling

Daikichi Mukoyama,[1] Toshiyuki Momma,[1,2] Hiroki Nara,[1] and Tetsuya Osaka*[1,2]
[1]*Research Institute for Science and Engineering, Waseda University, 3-4-1 Okubo, Shinjuku-ku, Tokyo 169-8555*
[2]*Department of Applied Chemistry, Faculty of Science and Engineering, Waseda University, 3-4-1 Okubo, Shinjuku-ku, Tokyo 169-8555*

(Received January 16, 2012; CL-120038; E-mail: osakatets@waseda.jp)

The degradation of the commercial Li ion battery was analyzed by electrochemical impedance spectroscopy, where our previous proposed equivalent circuit was applied. The degradation with the cycling was clearly explained by the main parameters of capacitive and resistive components, i.e., it responded until 300 cycles to the decrease in capacitive component, while after 300 to 550 cycles to the increase in resistive component.

A detection of the state of the degradation of batteries is one of the most important issues for energy storage systems. Electrochemical impedance spectroscopy (EIS) is the most effective method of nondestructive investigation for batteries. To detect the degradation using the EIS, efforts have been made by various groups.[1–4] We already proposed an equivalent circuit for a wide range of impedance spectra.[5] The equivalent circuit was newly redesigned for the analysis of the lithium ion battery (LIB) with consideration of the contributions of a variety of diffusion parameters resulting from the various particle sizes for the cathode and the solid-electrolyte interphase (SEI) formed on the anode particles, as well as electrochemical reactions and inductive components.[6] In addition, the sensitive assessment of residual errors resulting from the data fitting demonstrated the validity of the proposed circuit including the SEI component. The electrochemical impedance of the electrodes in a commercial LIB at various states of charge was analyzed to evaluate the proposed circuit.

In this study, we focused on an analysis using the impedance fitting technique on the basis of our previously proposed equivalent circuit for the degradation or the capacity fading of LIB with the charge–discharge cycling.

A commercially available prismatic LIB (Panasonic Corporation) with a nominal capacity of 850 mA h for cellular phones was used in this work. Active materials of anode and cathode were graphite and lithium cobaltite ($LiCoO_2$), respectively. The LIB was subjected to electrochemical tests at room temperature. The battery was charged and discharged with a constant current–constant voltage (CC–CV) protocol between 2.75 and 4.1 V at a rate of 1.0 C, after which it was maintained at this voltage for 3 h.

The ac impedance spectra at state of charge (SOC) 100% were obtained by measuring at an open-circuit voltage with 10 mV ac signal in the frequency range of 20 kHz to 0.2 mHz. All measurements were performed at room temperature. The data of the measured impedance were fitted with the equivalent circuit illustrated in Figure 1, which was proposed in ref 6.

Data fitting was carried out with Microsoft Excel Solver to reach the minimum value of the error, i.e., the sum of all the differences between the acquired experimental complex impedance data and the impedances calculated with the equivalent circuit using the parameters obtained by fitting for each frequency.

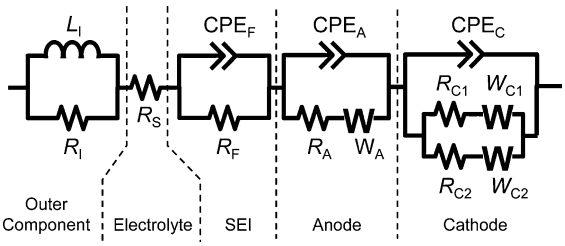

Figure 1. Equivalent circuit for fitting analysis of commercial LIB impedance. Symbols are expressed as follows: L_I, inductance of current collector and battery case; R_I, resistance of current collector; R_S, R_F, resistance of electrolyte and SEI; CPE_F, constant phase element of SEI; R_A, charge-transfer resistance of anode; CPE_A, CPE_C, constant phase element of electrode surface of anode and cathode; W_A, Warburg impedance for finite diffusion of anode. The cathode component including two particle size components is composed R_{C1}, R_{C2}, charge-transfer resistance; W_{C1}, W_{C2}, Warburg impedance for finite diffusion.

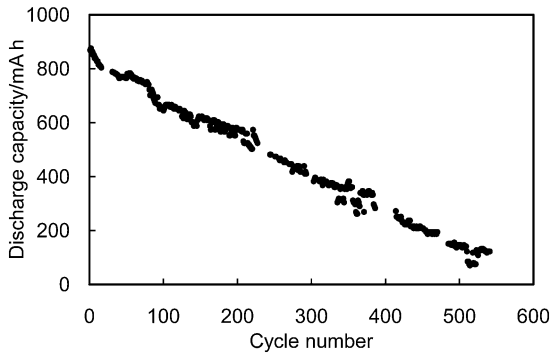

Figure 2. Battery discharge capacity with the number of charge–discharge cycles.

During continuous charge–discharge cycling of LIB, it was observed that the discharging capacity linearly faded with the cycling, as shown in Figure 2. The initial discharge capacity at the SOC of 100% is more than 850 mA h, and it gradually decreases to less than 200 mA h after 550 charge–discharge cycles at 1.0 C.

Typical fitting plots of the 10th and 550th cycle are illustrated with the data of the ac impedance responses in Figure 3. The dotted curve shows the impedance calculated

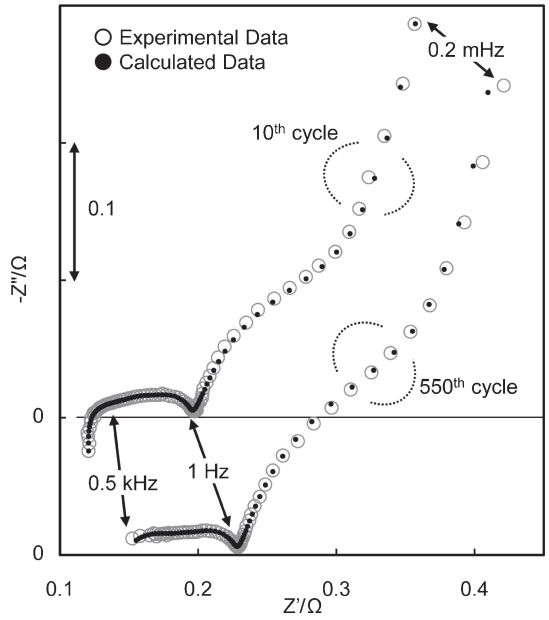

Figure 3. Typical fitting plots of experimental impedance spectra at SOC 100%. Plots between 0.2 kHz and 0.5 kHz at 550th cycle were excluded because of scattered experimental data obtained.

using the equivalent circuit. Until this study, the data of the low-frequency region were determined using the fitting technique including extrapolation and subtraction methods,[7] as shown in refs 5 and 6. The deviation between the experimental and calculated data in this low-frequency region could be considered negligible by using this extrapolation method. We succeeded in achieving a better fitting with the obtained data.

We previously assessed residual errors to the fitting in ref 6. The average values of residual errors in the impedance are given as less than 5 mΩ between 100 Hz and 1 mHz at all measuring points with the cycling, where the percentage of the error is approximately 1% to whole cell impedance obtained at 0.2 mHz. These errors are small enough to discuss the changing trend.

The fitting parameters for the 10th and 550th cycles obtained with the equivalent circuit, are shown in Table 1 as typical parameters. The CPE parameters can be expressed; $Z_{CPE} = 1/(j\omega)^p T$. When $p = 1$, the unit of T becomes Farad, a unit of capacitance. Parameters of the Warburg impedance are represented as follows; σ is the diffusion constant, C_L is the limiting capacitance.

The value of the limiting capacitance of whole cell was calculated by extrapolation in the low-frequency region plots, and is illustrated in Figure 4a. The limiting capacitance decreases until the 300th cycle and then becomes constant at 3.0 kF. The values of limiting capacitance obtained from fitting are shown in Figure 4b; those of cathodes 1 and 2 are 2.9 and 0.6 kF, respectively, decrease with an increase in the number of cycles. The capacitance of the anode is one order larger than that of the cathode and increases until the 300th cycle to 45 kF, after which it decreases to 18 kF at the 550th cycle. The limiting capacitance of the cathode is remarkably low compared with that of the anode. In LIB, electrodes were aligned in series along with the direction of current, and the lowest capacitance should

Table 1. Representative fitting parameters

Resistive parameter	Cycle 10th	Cycle 550th	Capacitive parameter	Cycle 10th	Cycle 550th
R_I/Ω	0.54	0.56	$L_I/\mu H$	0.22	0.21
R_S/Ω	0.12	0.15	p of CPE_F	0.57	0.73
$R_F/m\Omega$	35	43	T of CPE_F	0.32	0.15
$R_A/m\Omega$	23	12	p of CPE_A	0.85	1.0
$R_{C1}/m\Omega$	140	200	T of CPE_A	0.67	0.87
$R_{C2}/m\Omega$	22	31	p of CPE_C	1.0	0.97
			T of CPE_C	2.4	2.5
σ of W_A	6.1×10^{-3}	3.9×10^{-3}	C_L of W_A/kF	24	18
σ of W_{C1}	7.7×10^{-5}	1.5×10^{-4}	C_L of W_{C1}/kF	2.9	1.8
σ of W_{C2}	2.7×10^{-5}	1.1×10^{-4}	C_L of W_{C2}/kF	0.60	0.46

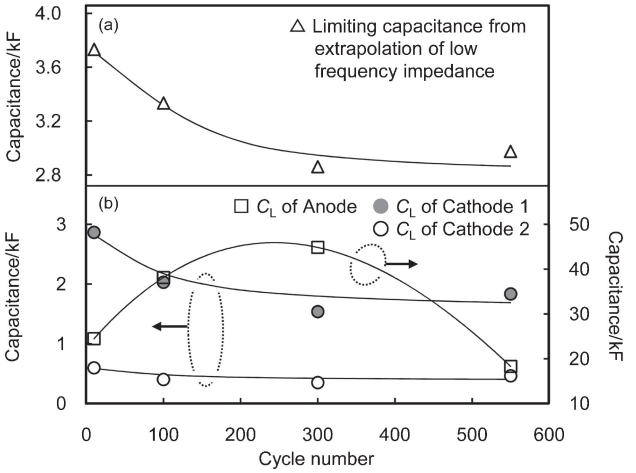

Figure 4. Variation of limiting capacitance with the number of charge–discharge cycles.

be the dominant. Therefore, the total limiting capacitance is regulated by the decreases of the limiting capacitance of the cathode with an increase in the number of cycles.

The whole resistances, which were represented as the real part of whole cell impedance obtained at 0.2 mHz, are 330–420 mΩ, as shown in Figure 5a. The voltage drop calculated from the whole resistance and the loading current of 1.0 C increased from 310 mV at the 10th cycle to 360 mV at the 550th cycle. Figure 5b shows the data of the resistive parameters fitted by the equivalent circuit with the number of charge–discharge cycles. The electrolyte resistance R_S increases from 120 mΩ at the 10th cycle to 150 mΩ at the 550th cycle. The diffusion resistance on the cathode component increased from 75 mΩ at the 10th cycle to 100 mΩ at the 550th cycle. With fitting results, we calculated individual diffusion resistances by subtraction.[7] The diffusion resistance of the anode component decreased from 122 to 59 mΩ at the 300th cycle and increased to 83 mΩ at the 550th cycle. From these results, it is clear that on diffusion, the increase in the resistive component R for the cathode corresponds to the increase in the entire resistance of the battery with increasing cycle number, whereas the resistance value for the anode decreases with the number of cycles. This implies that the diffusion on the cathode pores in the electrode degrades with an increase in the number of cycles when the diffusion length in the

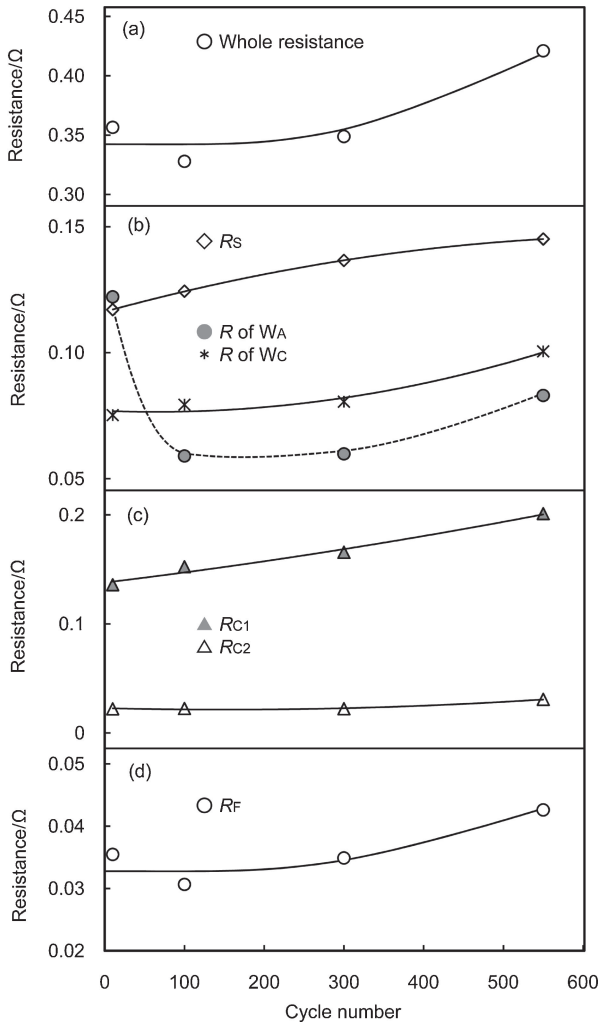

Figure 5. Variation of resistances with the number of charge–discharge cycles.

cathode is assumed to be almost constant. Barsoukov et al. investigated the kinetic properties of Li intercalation into $LiCoO_2$.[8] In their study, the increase of the diffusion resistance was reported to associate with blocking of a surface of the crystals of an active material, which interrupt the effective diffusion of Li^+. Further, they indicated that the decrease in the diffusion capacitance was due to the complete disconnection of some particle in the electrode. These conclusions agree well with our results.

The charge-transfer resistance of the cathode R_{C1} increases with cycle number, while that of R_{C2} remains nearly constant, as shown in Figure 5c. The value of R_{C1} was relatively high compared with that of R_{C2} while the total resistance, which was calculated as parallel connection of R_{C1} and R_{C2}, would be small. The charge-transfer resistance of the anode R_A slightly decreased with the cycle number (Table 1). These results suggest that the reaction rate at the anode is not changed drastically.

The SEI resistance, which is one order lower than the whole resistance, slightly increases with an increase in the number of cycles, as shown in Figure 5d. Yoshida et al. reported the mechanism of capacity fading in some batteries which was proposed to be an increase in the resistance of SEI.[9]

With continuous charge–discharge cycling of a prismatic commercial LIB for cellular phones, the discharge capacity was demonstrated to be fading. During the capacity fading with charge–discharge cycling until the fade of 550th cycling, the capacity of the cathode was revealed to decrease until the 300th cycling, and after that, the internal resistance of the whole cell was found to increase. These results indicate that the analysis with the proposed equivalent circuit enabled interpretation the battery impedance behavior measured with the two-electrode system for a wide range of frequencies, and it exactly provides this method as the proper analysis tool for the study of capacity fading.

This work was supported by "Research & Development Initiative for Scientific Innovation of New Generation Batteries" from the New Energy and Industrial Technology Development Organization (NEDO) of Japan and a Grant-in-Aid for Specially Promoted Research "Establishment of Electrochemical Device Engineering" from the Ministry of Education, Culture, Sports, Science and Technology, Japan (MEXT) and done in the Center for Practical Chemical Wisdom of Global COE.

References

1 D. Zhang, B. S. Haran, A. Durairajan, R. E. White, Y. Podrazhansky, B. N. Popov, *J. Power Sources* **2000**, *91*, 122.
2 J. Li, E. Murphy, J. Winnick, P. A. Kohl, *J. Power Sources* **2001**, *102*, 294.
3 J. P. Zheng, P. L. Moss, R. Fu, Z. Ma, Y. Xin, G. Au, E. J. Plichta, *J. Power Sources* **2005**, *146*, 753.
4 Y. Zhang, C.-Y. Wang, X. Tang, *J. Power Sources* **2011**, *196*, 1513.
5 T. Osaka, S. Nakade, M. Rajamäki, T. Momma, *J. Power Sources* **2003**, *119–121*, 929.
6 T. Osaka, T. Momma, D. Mukoyama, H. Nara, *J. Power Sources* **2012**, *205*, 483.
7 T. Osaka, N. Oyama, T. Ohsaka, *Electrochemical Measurement: Basic Manual*, 7th ed., Kodansha-Scientific, Tokyo, **1994**.
8 E. Barsoukov, D. H. Kim, H.-S. Lee, H. Lee, M. Yakovleva, Y. Gao, J. F. Engel, *Solid State Ionics* **2003**, *161*, 19.
9 T. Yoshida, M. Takahashi, S. Morikawa, C. Ihara, H. Katsukawa, T. Shiratsuchi, J.-i. Yamaki, *J. Electrochem. Soc.* **2006**, *153*, A576.

